

## OPTICAL PHENOMENA ASSOCIATED WITH BRAZIL-TWIN BOUNDARIES IN QUARTZ

A. SPRY, R. G. TURNER AND R. C. TOBIN,  
*Physics Department, Monash University, Clayton, Victoria 3168,  
Australia.*

### ABSTRACT

Brazil-twin (left-handed to right-handed) boundaries in quartz when viewed between crossed polarizers under the microscope are marked by dark fringes. Complexities due to undulations on the twin boundary, to multiple parallel and intersecting twin boundaries and to tilting of the section may be recognized. The fringes are the result of optical activity and arise from the interference of elliptically polarized *ordinary* and *extraordinary* waves. Fringes are visible in thick sections but become more difficult to observe as the thickness is reduced; in petrographic thin sections (0.03 mm), those due to single and multiple boundaries are visible but those due to tilting are not.

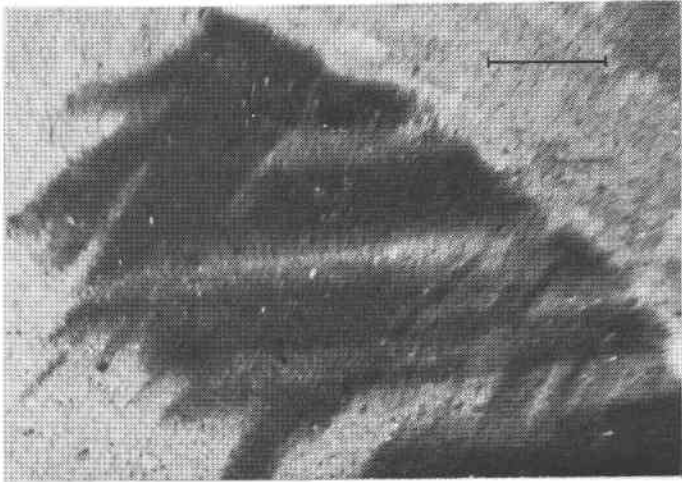
### INTRODUCTION

A Brazil twin in quartz consists of a left-handed region and a right-handed region in contact (Fron del, 1962, pp. 87-90). On the macroscopic scale the twin boundary may be planar or undulating but, ultimately, all boundaries consist of planar segments. The most common planes are  $\{10\bar{1}1\}$  and  $\{\bar{1}011\}$  with  $\{12\bar{1}1\}$ ,  $\{2\bar{1}11\}$ ,  $\{01\bar{1}0\}$ ,  $\{1\bar{1}00\}$ ,  $\{2110\}$  and  $\{0001\}$  being much less common.

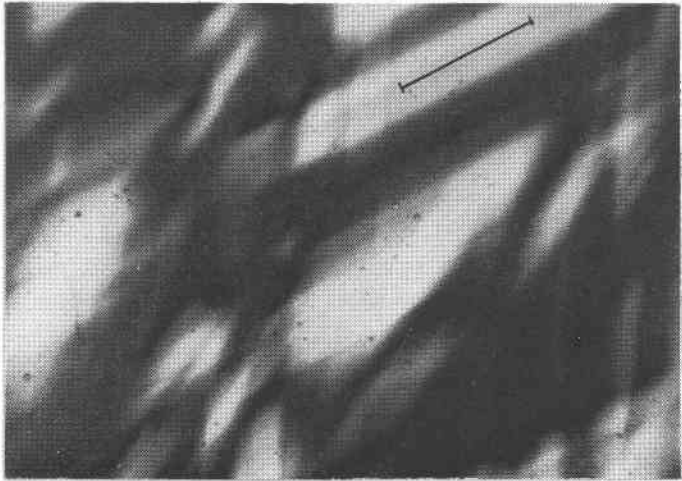
Brazil twins have been extensively studied in quartz used for oscillator plates (Vigoureux and Booth, 1950), where twinning precludes the use of some crystals, but have been neglected by the mineralogist and petrologist for two reasons. First, they are rare in quartz other than that formed in veins, and second, they are commonly believed to be invisible in normal thin sections (0.03 mm). Two sets of multiple intersecting Brazil twins in Figure 1a are clearly visible in a normal thin section.

Work in the past has been largely confined to viewing thick basal slices (e.g. a Z-cut oscillator plate) at normal incidence between crossed polarizers (Vigoureux and Booth, 1950). The  $\{10\bar{1}1\}$  and  $\{\bar{1}011\}$  twin-boundaries are then inclined at about  $52^\circ$  to the slices and each boundary is marked by a single dark fringe where light traverses equal thicknesses of right-handed and left-handed crystal.

It does not appear to be appreciated, however, that: (1) An undulating boundary gives rise to a fringe structure which depends on the profile of the boundary (profile-controlled fringes), (2) Fringes on twin-boundaries are visible in nonbasal sections (tilt-controlled fringes), (3) Multiple parallel and intersecting twins are marked by multiple and intersecting fringe systems, and (4) Single twin-boundaries are visible in normal petrographic thin-sections.



(a)



(b)

FIG. 1. Multiple intersecting Brazil twins viewed in basal slices. (a) In a normal thin section (0.03 mm thickness) with the analyzer rotated clockwise  $3^\circ$  so that right-handed regions are dark and left-handed are bright. Twins parallel to  $(10\bar{1}1)$  and  $(\bar{1}101)$  end at a grain boundary in the upper right. The scale bar is 0.2 mm. (b) In a 0.5-mm slice with crossed polarizers. Two sets of dark fringes intersecting at  $60^\circ$  are parallel to  $(10\bar{1}1)$  and  $(\bar{1}101)$  but additional oblique dark and bright streaks occur at intersections of twins and bisect the  $60^\circ$  intersection angle (see Fig. 9). The scale-bar is 0.5 mm.

The above fringes are described and it is shown that they arise because of the optical activity of quartz.

#### OBSERVATIONS

The specimens were in the form of basal slices (perpendicular to the optic axis), of thickness about 0.5 mm, mounted on a universal stage on a petrographic microscope with its polarizer and analyzer crossed. Observations oblique to the optic axis were made by rotating the slices about the horizontal axis and tilt-controlled fringes were only visible when this horizontal axis was parallel to the polarizing direction of either the polarizer or analyzer. Refraction and reflection at the faces of the specimen were made negligible by surrounding it with an oil of matching refractive index between matching glass hemispheres. Complications due to the dispersion of the optical properties of quartz were avoided by illuminating through a narrow-band optical filter.

*Planar boundary viewed along the optic axis.* A single dark fringe is visible at the centre of an inclined planar Brazil-twin boundary (Fig. 2a). Rotation of the analyzer through a small angle increases the illumination on one side of the boundary and reduces it on the other side, the dark fringe moving towards the side of reduced illumination.

*Undulating boundary viewed along the optic axis.* An undulating boundary is marked by a fringe system consisting of a central dark major fringe with a fine structure of parallel minor fringes (Fig. 2b). Rotation of the analyzer through a small angle causes movement of the central major fringe. The minor fringes do not change position with rotation of the analyzer but reverse contrast as the major fringe passes across them.

These profile-controlled fringes can be correlated in position with undulations of the twin-boundary which is revealed by grinding a section across the boundary, etching in HF and viewing under a microscope (Figs. 2d, 5).

*Planar boundary viewed obliquely to the optic axis.* The single dark fringe observed when a planar boundary is viewed along the optic axis is replaced by a system of fringes which appears as follows. As the tilt is progressively increased from zero the field is alternately uniformly bright and dark with a number of parallel bright fringes along the twin boundary. On each successive appearance of the fringes their number is increased by one. Thus, for a slice 0.5 mm thick, the single dark fringe visible at zero tilt (Fig. 2a) is replaced, at a tilt of  $10^\circ$ , by a uniformly illuminated field. At  $15^\circ$  the field is dark except for a single

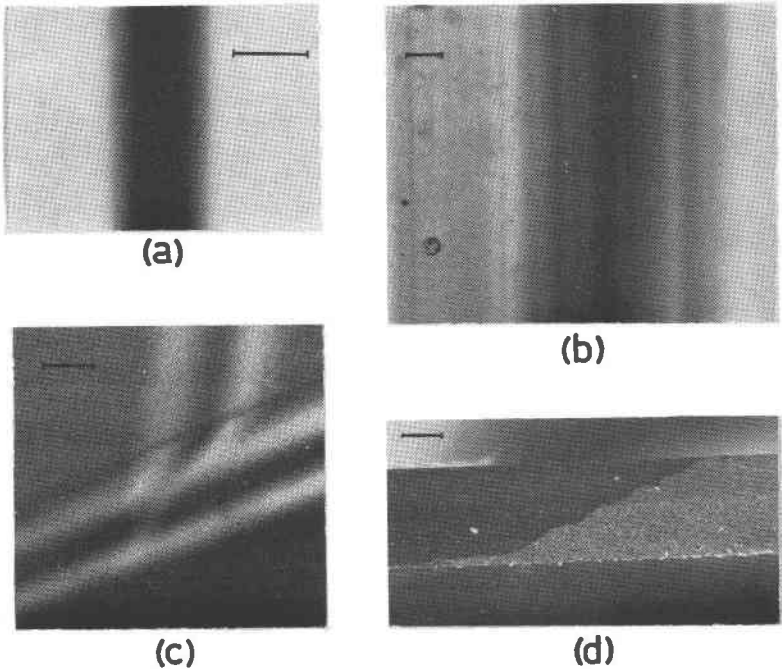


FIG. 2. Single and multiple fringes on twin boundaries. Scale-bar is 0.2 mm in each case. (a) Single dark fringe on an inclined planar Brazil-twin boundary in a 0.65-mm basal slice of quartz viewed along the optic axis. Left-handed to the left of the fringe, right-handed to the right, crossed polarizers. Further data on Fig. 4. (b) Profile-controlled fringes on the inclined undulating twin-boundary (Fig. 2d and 5) in a 0.65-mm basal slice viewed along the optic axis. Crossed polarizers. Compare with Fig. 2d. (c) 0.5-mm basal slice tilted at  $24^\circ$  on the universal stage. Crossed polarizers. Two bright fringes on the twin boundary (upper part of figure) meet two bright fringes on the wedge-shaped edge of the slice (lower part of figure). See text. (d) Cross-section of a 0.65-mm basal slice of quartz with the undulating twin-boundary revealed by reflected light from an etched surface. Orientation corresponds to (b) above and Fig. 5.

bright fringe along the boundary. At  $20^\circ$  the field again becomes uniformly light and, at  $24^\circ$ , dark but with two bright fringes (upper part of Fig. 2c). This sequence continues, thus at  $28^\circ$  there are three bright fringes, at  $32^\circ$  four bright fringes and at  $36^\circ$  five bright fringes, in each case on a dark background.

If the junction between an external edge of the specimen and an internal Brazil-twin boundary is viewed at various angles of tilt the same number of fringes appears on each (Fig. 2c).

*Multiple parallel boundaries.* A group of parallel, inclined, closely spaced boundaries viewed along the optic axis is marked by a complex as-

semblage of parallel fringes. Each twin boundary also produces the tilt-controlled fringes described earlier when the slice is tilted and a multiply-twinned region may be recognized by the complex and irregular series of parallel fringes which cover it on tilting.

*Intersecting multiple boundaries.* The fringes described above are all parallel to the traces of the twin boundaries on the basal plane. Figure 1b, however, shows a typical example in which two intersecting systems of parallel twin-boundaries which are equally inclined to the optic axis produce, in addition, fringes which bisect the angle between the traces of the twin boundaries on the surface of the slice.

#### *Optical activity in quartz*

General discussions of optical activity are given in standard texts such as Jenkins & White (1957), Nye (1957) and Shubnikov (1960) but no attempt seems to have been made to apply optical theory to an explanation of the optical phenomena associated with Brazil twin boundaries. As optical activity is a topic which is neglected by most mineralogists, explanations of the optical phenomena are developed from first principles.

If a linearly (plane-) polarized plane light wave is transmitted along the optic axis of quartz, the plane of polarization is rotated through an angle  $\phi$  which is proportional to the distance  $d$  travelled by the light wave in the crystal. Thus

$$\phi = \rho d \quad (1)$$

$\rho$  is the specific rotation which ranges from  $48.945^\circ/\text{mm}$  for  $4046.56 \text{ \AA}$  to  $11.589^\circ/\text{mm}$  for  $7947.63 \text{ \AA}$  (Jenkins and White, 1957).

This effect can be understood by considering the incident linearly-polarized wave to consist of two circularly-polarized waves of equal amplitude but of opposite hand. The convention is that a circularly polarized wave whose electric vector rotates clockwise as seen by an observer whose eye the light is entering is termed right handed. The resolution into circularly polarized waves is chosen because they are the only waves which propagate along the optic axis of quartz with their states of polarization unchanged. The refractive index of the quartz differs for these two waves which consequently emerge with a phase-difference  $\alpha$ .

$$\beta = 2\pi \frac{d}{\lambda} (n_l - n_r) \quad (2)$$

where  $n_l$  and  $n_r$  are respectively the refractive indices for the left-handed and right-handed circularly polarized waves and  $\lambda$  is the wavelength of

the light in vacuum. The superposition of the two emergent circularly-polarized waves gives a linearly-polarized wave with its plane of polarization rotated through the angle  $\phi$  which is equal to  $\alpha/2$ . Thus

$$\beta = \pi \frac{(n_1 - n_r) d}{\lambda} \quad (3)$$

and so

$$\rho = \pi \frac{(n_1 - n_r)}{\lambda} \quad (4)$$

Right-handed and left-handed quartz rotate the plane of polarization in clockwise and anticlockwise directions respectively, as seen by an observer whose eye the light is entering.

When light is transmitted through a nonbasal section oblique to the optic axis, again only two waves can propagate with their states of polarization unchanged. These are elliptically polarized, have the same ellipticity  $k$  (ratio of minor to major axis), are of opposite hand and travel with different speeds. The major axes of the electric-vector ellipses are mutually perpendicular and lie along the principal vibration (electric-vector) directions which would exist for this direction of the wave-normal in the absence of optical activity. The quartz would then be merely birefringent and the elliptically polarized waves would degenerate into the familiar ordinary and extraordinary waves. By analogy, the elliptically polarized waves which occur in quartz will be called *ordinary* or *extraordinary* when their major axis lies along the electric-vector direction of the ordinary or the extraordinary wave respectively of the purely birefringent case. This distinction is lost for propagation along the optic axis, both waves then being circularly polarized.

The ellipticity of the two waves is thus unity for propagation along the optic axis and decreases rapidly as the wave-normal makes an increasing angle with the optic axis (Nye, 1957, Fig. 14.3). The ellipticity becomes zero for directions of the wave-normal making an angle of  $56^\circ 10'$  with the optic axis. For angles greater than  $56^\circ 10'$  the ellipticity increases with angle but the *ordinary* and *extraordinary* waves interchange hand.

In right-handed quartz the *ordinary* wave is right-handed for directions of the wave-normal making angles of less than  $56^\circ 10'$  with the optic axis. For a given direction of the wave-normal the refractive index,  $n_o$ , for the *ordinary* wave is the same for both right-handed and left-handed quartz but the elliptically-polarized waves are of opposite hand. A similar statement holds for the *extraordinary* wave, the refractive index being denoted by  $n_e$ .

Thus a linearly polarized wave entering a quartz crystal will, even if polarized in a principal plane, in general excite two elliptically polarized waves which travel at different speeds. The superposition of these waves on emerging produces the observed fringes.

Optical activity is essential for the production of fringes because in each case described the optic axis of the quartz slice lies in the plane of polarization of either the polarizer or the analyzer. If the crystal were nonactive and birefringent then the wave excited in the slice would then be either wholly extraordinary or ordinary (linearly polarized), it would emerge without rotation of its plane of polarization and consequently would be extinguished by the analyzer and the crystal would always appear uniformly dark. Any fringes which are observed in quartz must therefore arise through optical activity. The fringe systems seen in tilted basal slices show that phenomena due to optical activity are observed for directions of the wave-normal which make large angles with the optic axis.

#### EXPLANATIONS OF OBSERVATIONS

*Inclined boundary viewed along the optic axis.* A typical light path  $AB$  which crosses an inclined boundary in a basal slice is depicted in Figure 3a and the amplitude of the incident linearly-polarized wave is denoted by  $E_m$ . The net clockwise rotation  $\phi$  of the plane of polarization (which

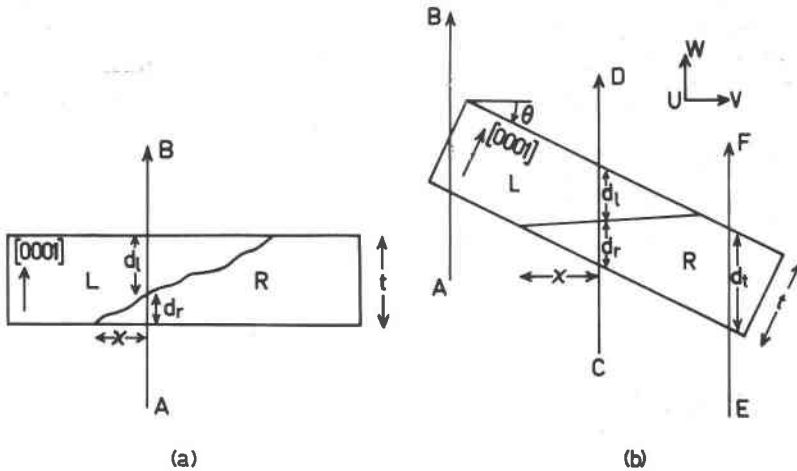


FIG. 3. Ray paths in crystal slices. (a) Ray path  $AB$  parallel to the optic axis through a basal slice containing a Brazil-twin boundary.  $L$  and  $R$  mark left-handed and right-handed regions respectively. (b) Ray paths through a tilted basal slice containing a planar Brazil-twin boundary.  $U, V, W$  are reference axes which are fixed with respect to the microscope.

may be measured by rotating the analyzer to extinction) is  $\rho(d_r - d_l)$  where  $d_r$  and  $d_l$  are the distances travelled through right-handed and left-handed quartz respectively. The component of the electric vector transmitted by the analyzer is  $E_m \sin[\rho(d_r - d_l)]$  if losses are assumed to be negligible. The square of the transmitted electric vector will be referred to in this paper as the intensity  $I$ . In this case

$$I = E_m^2 \sin^2[\rho(d_r - d_l)]. \quad (5)$$

$(d_r - d_l)$  ranges from  $-t$  to  $+t$  where  $t$  is the thickness of the quartz slice and, for slices of thickness about 0.5 mm,  $\rho t$  is about  $10^\circ$ . When the analyzer is rotated through the angle  $\psi$  (clockwise viewed from above) the intensity is given by

$$I = E_m^2 \sin^2[\rho(d_r - d_l) - \psi]. \quad (6)$$

*Planar boundary.* Within the boundary region,  $(d_r - d_l)$  changes linearly with  $\chi$ , the horizontal distance from the intersection of the boundary with the lower face. There is a central dark fringe at the point where  $(d_r - d_l) = 0$ , *i.e.*  $d_r = d_l$  and the total clockwise rotation equals the anti-clockwise rotation. The intensity rises symmetrically on each side of this point up to the constant value  $E_m^2 \sin^2 \rho t$  which it has outside the boundary region.

Figure 4 shows a comparison between a set of experimental points derived from the negative of Figure 2a and the intensity curve computed from Eq. (5). The slight discrepancy at low intensities occurs because the relationship between density in the photographic plate and log intensity was assumed linear in deriving intensity values from the microdensitometer trace. This assumption fails for low photographic densities.

When the analyzer is rotated through the angle  $\psi$ , Eq. (6) shows that the intensity on one side of the boundary region becomes  $E_m^2 \sin^2(\rho t - \psi)$  and that on the other side  $E_m^2 \sin^2(\rho t + \psi)$  and the dark fringe moves towards the side of reduced intensity.

*Undulating boundary.* If the profile of the boundary is given by

$$d_r = f(\chi) \quad (7)$$

then the intensity is (from Eq. (5))

$$I = E_m^2 \sin^2 \left\{ 2\rho \left[ f(\chi) - \frac{t}{2} \right] \right\}. \quad (8)$$

The variation in intensity (*i.e.* the fringe pattern) reflects the profile of the boundary. Figure 5 shows the correlation between the profile of the

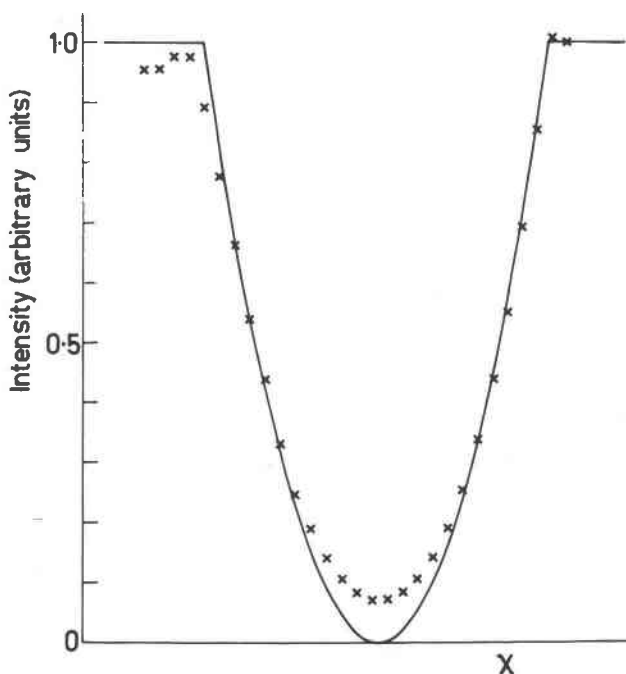


FIG. 4. Comparison—measured values (denoted by x) and theoretical values predicted by Eq. (5) (solid curve) for the transmitted intensity across a fringe due to an inclined planar boundary viewed along the optic axis between crossed polarizers. The discrepancy at low intensities is due to the assumption of a linear characteristic for the photographic material in deriving the intensity values.

boundary of Figure 2b and the microdensitometer trace of the fringe pattern of Figure 2d. A 0.001-mm undulation can be readily recognized from the densitometer trace and some refinement of technique may allow smaller undulations to be detected.

Figure 6b shows a plot of  $\phi$  (which is equal to  $2\rho[f(\chi) - t/2]$ ) as a function of  $\chi$  across the inclined boundary with a single undulation shown in Figure 6a. The intensity of the light (which is proportional to  $\sin^2 \phi$ ) transmitted by the analyzer is shown as curve A in Figure 6c. A light or dark minor fringe is the result of a small fluctuation in  $\phi$ , which, in turn, results from a fluctuation in the difference of thicknesses of quartz of either hand traversed by the light (*i.e.*  $d_r - d_l$ ). Rotation of the analyzer from the crossed position through an angle  $\psi$  makes  $I$  proportional to  $\sin^2(\phi - \psi)$  (see Eq. (6)). Figure 6c (curve B) shows how this has the effect of replacing the light fringe at D by a dark fringe. Thus as the analyzer is rotated the major dark fringe, where  $\phi - \psi = 0$ ,

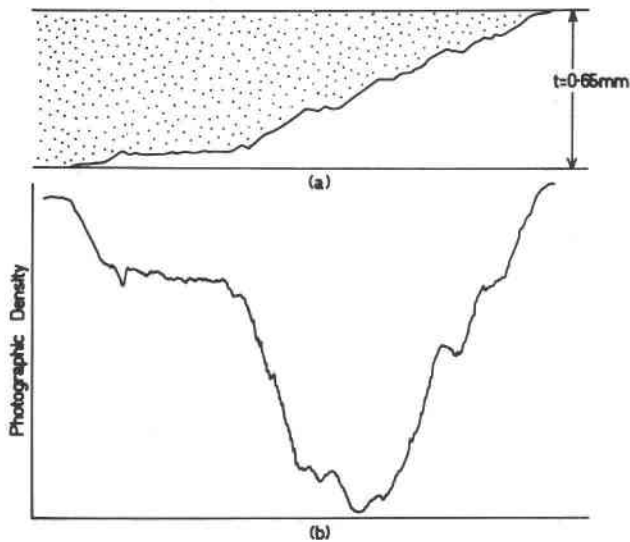


FIG. 5. Comparison of twin-boundary shape and profile-controlled fringes. (a) The undulating boundary of Fig. 2d. (b) Microdensitometer traverse across a photomicrograph of the fringe system due to this boundary (Fig. 2b). The point of zero intensity occurs where the light path traverses equal thicknesses of left-handed and right-handed material. The fluctuations can be correlated with "steps" or undulations on the boundary in (a). [The horizontal scales of (a) and (b) are the same.]

moves sideways across the boundary region from  $X$  to  $Y$  and the minor fringes reverse contrast as the major fringe crosses them.

*Planar inclined boundary viewed obliquely to the optic axis.* The orientation of the specimen is referred to the orthogonal coordinate axes  $UVW$  (Figure 3b) where  $W$  is parallel to the vertical axis of the microscope and  $V$  is parallel to the electric vector of the light incident on the specimen (*i.e.* to the plane of polarization of the polarizer). It is assumed that the polarizer and analyzer are crossed and that the specimen is tilted about the  $U$  axis. The results are unchanged if the specimen is, instead, tilted about the  $V$  axis. The *ordinary* and *extraordinary* waves which are excited just within the first face of the slice are the same for the paths  $AB$ ,  $CD$  and  $EF$ , except that the hands of the elliptical vibrations in  $AB$  are the reverse of those in  $CD$  and  $EF$ . It will be assumed that the *ordinary* and *extraordinary* waves have a common wave-normal and that the electric vectors of both are perpendicular to their wave-normal. Reflection and deviation of the waves at all boundaries are ignored. An exact analysis shows that these assumptions do not significantly affect the results.

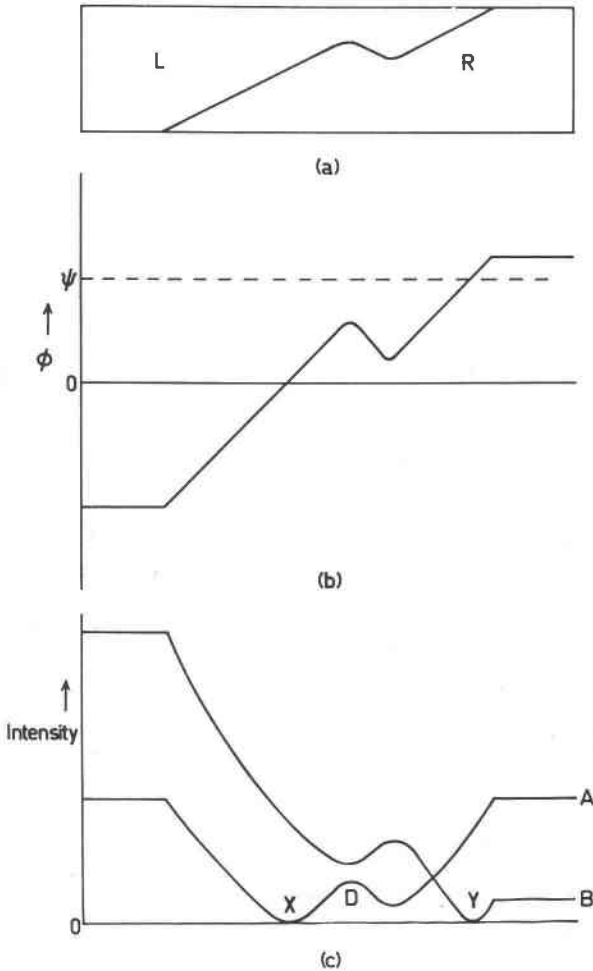


FIG. 6. Movement of profile-controlled fringes on rotating the analyzer. (a) Schematic diagram of a basal slice containing a Brazil-twin boundary with a single undulation. (b) Graph of  $\phi$ , the angle of rotation of the plane of polarization of linearly polarized light, travelling parallel to the optic axis, due to passage through the slice. (c) The transmitted intensity with polarizers crossed (curve A). Rotation of the analyzer through an angle  $\psi$  from the crossed position causes the position of zero intensity to move laterally and the minor fringes to reverse contrast (curve B).

Just inside the first face the resultant electric vector must equal that of the incident wave, which always lies in the  $V$  direction of the coordinate axes of Figure 3b. In order that the resultant  $U$ -component be zero the  $U$ -components of the *ordinary* and *extraordinary* waves must be of the same amplitude and differ in phase by  $\pi$ . This means that the

major axis of the ellipse representing the *ordinary* wave must equal the minor axis of the ellipse representing the *extraordinary* wave.

Consider the paths AB and EF in Figure 3b. The *ordinary* and *extraordinary* waves travel through the quartz with different speeds (the *ordinary* wave being the faster of the two) so that they arrive at the exit boundary having travelled a distance  $d$  with their  $U$ -components differing in phase by  $\pi - \beta$  where

$$\beta = 2\sigma d \quad (9)$$

$\sigma = \pi[(n_0 - n_e)/\lambda]$ . The quantity  $\sigma$  must be distinguished from the specific rotation  $\rho$ . The component transmitted by the analyzer is the resultant  $U$ -component, which is, in general, not zero. The transmitted intensity is

$$I = 4 \left( \frac{k}{1 + k^2} \right)^2 E_m^2 \sin^2 \sigma d \quad (10)$$

EF in Figure 3b is a typical path in the region of constant thickness in which the slice is wholly right-handed. In this case  $d = d_t = t/\cos \theta$  ( $\theta$  being the angle of tilt) which is constant for a given  $\theta$  and so this region will appear uniformly illuminated. A similar conclusion holds for a path in a wholly left-handed region of constant thickness. As  $\theta$  is increased the variation in the illumination of such regions is due mainly to the oscillatory behaviour of  $\sin^2 \sigma d_t$ , which, in turn, arises mainly from the increase in  $(n_0 - n_e)$ . The transmitted intensity is zero when

$$\sigma d_t = m\pi \quad (11)$$

where  $m$  is an integer.

AB is a typical path in the wedge-shaped edge-region of the slice. At a given value of  $\theta$ ,  $d$  varies uniformly from 0 to  $t/\cos \theta$  and a fringe system is observed. In particular, when  $\theta$  is such that Eq. (11) is satisfied with a particular integer  $m$ , there are  $m$  complete fringes over the region of the wedge.

The path CD (Fig. 3b) crosses the Brazil-twin boundary and passes through thickness  $d_r$  and  $d_l$  of right-handed and left-handed quartz respectively. After travelling  $d_r$  the resultant field,  $E$ , of the *ordinary* and *extraordinary* waves possesses  $U$  and  $V$ -components  $E_U$  and  $E_V$  respectively which in general are not zero. These two components each, separately, give rise to a pair of *ordinary* and *extraordinary* waves as they pass into the left-handed region at the twin boundary. The four elliptically polarized waves then travel a distance  $d_l$  in the left-handed region. Qualitatively it can be seen that the wave emerging from the slice will, in general, have a nonzero  $U$ -component which is transmitted

by the analyzer. An analysis shows that the transmitted intensity is given by

$$I = 4 \frac{k^2}{(1+k^2)^4} E_m^2 \{ [1-k^2]^2 [1-2 \cos \sigma d_t \cdot \cos[\sigma(d_r-d_l)] + \cos^2 \sigma d_t] + 4k^2 \sin^2[\sigma(d_r-d_l)] \}. \quad (12)$$

When  $k=1$ , that is for propagation along the optic axis, Eq. (12) reduces to Eq. (5). To obtain a tractable expression for other directions of the wave-normal the approximation is made that all terms of higher powers than the first in  $k^2$  are neglected. Since  $k^2$  falls to about 0.1 when  $\theta=8^\circ$  a careful study of the exact expression shows that no essential detail is lost by this approximation for  $\theta$  greater than  $8^\circ$ . The approximate form of Eq. (12) is

$$I = 4k^2 E_m^2 \{ 1 + \cos^2 \sigma d_t - 2 \cos \sigma d_t \cos[\sigma(d_r-d_l)] \}. \quad (13)$$

At a fixed value of  $\theta$ ,  $\cos \sigma d_t$  does not vary over the region of constant thickness of the slice. It is the factor  $\cos[\sigma(d_r-d_l)]$  which is responsible for the observed fringes. The visibility of the fringes is maximum when  $\sigma d_t = m\pi$  which is precisely the condition (Eq. (11)) for the region outside the boundary to be dark. When this condition is satisfied Eq. (13) reduces to

$$I = 16k^2 E_m^2 \sin^2(\sigma d_r). \quad (14)$$

Thus, when  $\sigma d_t = m\pi$ , the fringe system consists of  $m$  bright fringes on a dark background.

Figure 7 shows the variations in intensity in the fringe system at  $\theta$  equal to zero and at successive value of  $\theta$  for which the fringe visibility is maximum. Equation (14) closely resembles Eq. (10), and when Eq. (10) is applied to the wedge-shaped edge region, the ranges of  $d$  in Eq. (10) and  $d_r$  in Eq. (14) are the same, that is 0 to  $t/\cos \theta$ . Hence, for a tilt angle  $\theta$  giving maximum fringe visibility, there are as many fringes visible at the edge of the slice as there are over the region of the inclined boundary (see Fig. 2c).

The fringe visibility is zero when  $\sigma d_t = (m + \frac{1}{2})\pi$ , and this condition coincides with that for maximum illumination outside the boundary region. When this condition is imposed on Eq. (13), the intensity is everywhere equal to  $4k^2 E_m^2$ .

*Multiple parallel boundaries.* Irregular parallel fringes are produced by closely spaced multiple twins (e.g. lower right of Fig. 1a and centre of Fig. 1b). Schematic curves showing the variations in intensity across

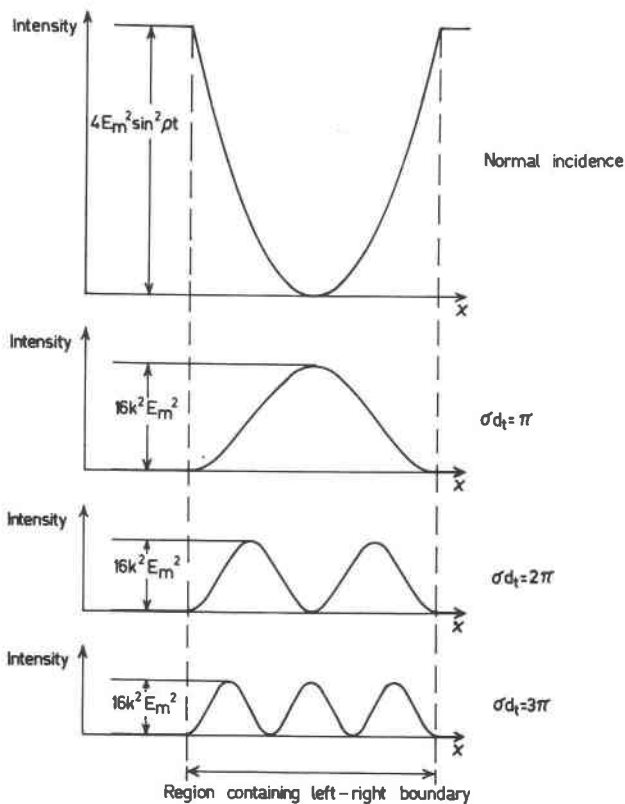


FIG. 7. Intensity in the fringe system due to an inclined planar Brazil-twin boundary viewed along the optic axis and at successive angles of tilt for which the fringe visibility is maximum. The diagram, from top to bottom, shows one dark fringe at zero tilt and successively one, two and three bright fringes on a dark background.

some typical multiple parallel Brazil-twin boundaries shown in Fig. 8 have been deduced by applying the argument given for the single inclined boundary viewed along the optic axis. Although it is possible to recognize optically that a region in a slice contains a number of parallel inclined boundaries it is difficult to infer the exact nature of the twinned structure from the intensity curve.

*Intersecting multiple boundaries.* Sections of quartz commonly contain two sets of Brazil-twin boundaries parallel to  $\{10\bar{1}1\}$  and/or  $\{01\bar{1}1\}$  whose traces on the basal plane are at  $60^\circ$  to each other (Figs. 1a and 1b). Where the boundaries can be viewed separately along the optic axis each will be marked by a single dark fringe where the light traverses

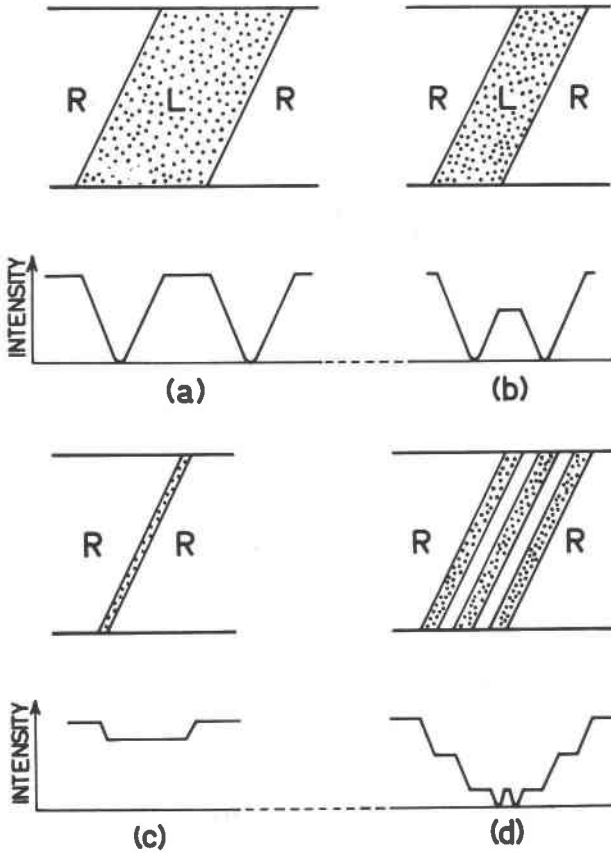


FIG. 8. Schematic intensity variations in the fringe systems produced when basal slices containing various multiple parallel planar twin-boundaries are viewed along the optic axis between crossed polarizers.

equal thicknesses of left-handed and right-handed quartz. However, where the boundaries intersect, there are regions of complex overlap of left-handed and right-handed quartz. For a given geometry of the intersecting boundaries the resulting fringes can be inferred by applying the argument given for the single inclined boundary viewed along the optic axis. The broad features of the fringe system due to multiple intersecting boundaries can be understood by consideration of the simplest case, that of two intersecting boundaries (Fig. 9a). Figure 9b is a plan view showing the traces of the boundaries on the upper and lower surfaces of the basal slice. Normal fringes due to single boundaries occur outside the central region WXYZ. Inside this region dark fringes

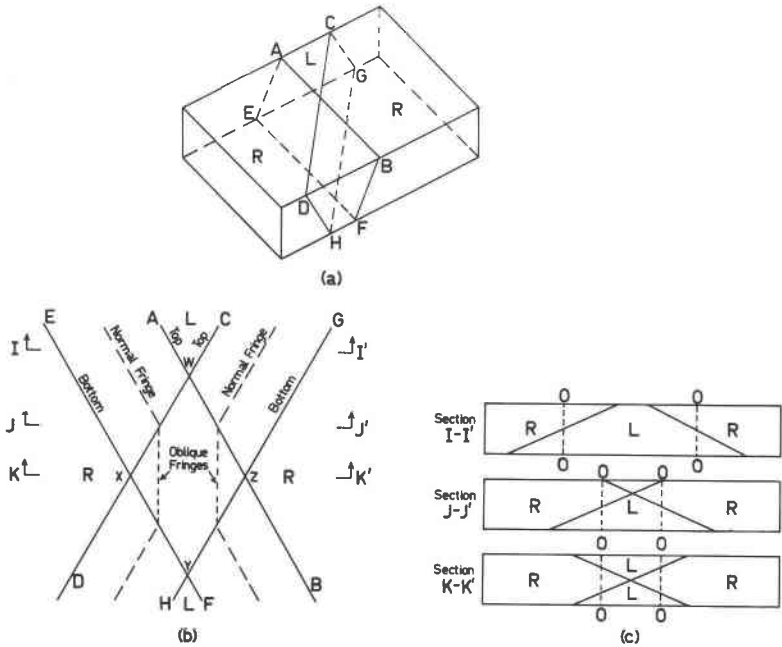


Fig. 9. Fringes on multiple inclined intersecting boundaries. (a) Diagram showing two intersecting twin-boundaries in a basal slice. (b) Plan view of (a) showing the traces of the twin boundaries on the top of the slice ( $AB$  and  $CD$ ) and on the bottom of the slice ( $EF$  and  $GH$ ). (c) Cross-section of the slice along lines  $II'$ ,  $JJ'$  and  $KK'$  in (b) showing the overlap of left-handed ( $L$ ) and right-handed ( $R$ ) regions. Light paths which traverse equal thicknesses of left-handed and right-handed quartz are marked  $OO$ .

appear along loci for which the light traverses equal thicknesses of left-handed and right-handed quartz. It can be seen, from the sections  $JJ'$  and  $KK'$  shown in Figure 9c, that these fringes bisect the acute angle between the normal fringes as shown in Figure 9b. In general these oblique fringes bisect either the acute or the obtuse angle between the normal fringes on the boundaries since they are parallel to the projection of the line of intersection of the boundaries on the surface of the slice. A region of intersecting multiple twin-boundaries will be marked by normal fringes parallel to the twin boundaries, oblique fringes at their intersections, and diamond-shaped bright areas whose long axes bisect the acute angle between the normal fringes (see Fig. 1b).

#### FRINGES IN PETROGRAPHIC THIN SECTIONS

It is generally considered (Fron del, 1962, p. 89) that a Brazil twin is not noticeable in a normal petrographic thin section of 0.03 mm thick-

ness when viewed along the optic axis because of the small optical rotation (about  $0.6^\circ$ ). The dark fringe is certainly difficult to see between crossed polarizers because it is very narrow and the level of illumination on each side is very low, but the two parts of the twin become unequally illuminated and the boundary clearly visible when the analyzer or polarizer is rotated by a few degrees (Fig. 1a).

Profile-controlled fringes caused by undulations of the twin boundary of a few micrometers are again very difficult to see in normal thin sections between crossed polarizers due to the general low level of illumination. Rotation of the analyzer or polarizer by a few degrees brightens the field and enables the minor fringes to be seen.

Tilt-controlled fringes cannot be seen in normal thin sections since the angle of tilt for the first bright fringe becomes impractically high for sections less than about 0.1 mm in thickness.

The oblique fringes produced at the intersection of inclined and intersecting multiple twin-boundaries are extremely difficult to see in thin sections because of the small areas of overlap of the boundaries and because of the general low level of illumination.

#### REFERENCES

- FRONDEL, C. (1962) *The system of Mineralogy . . .*, Vol. III, *Silica Minerals*. John Wiley and Sons, New York.
- JENKINS, F. A., AND H. E. WHITE (1957) *Fundamentals of Optics*. McGraw-Hill, New York.
- NYE, J. F. (1957) *Physical Properties of Crystals*. Clarendon, Oxford.
- SHUBNIKOV, A. V. (1958) *Principles of Optical Crystallography*. [Transl. Consultants Bureau, New York, 1960.
- VIGOUREUX, P., AND C. F. BOOTH (1950) *Quartz Vibrators*. H. M. Stationary Office, London

*Manuscript received, May 14, 1968; accepted for publication, July 2, 1968.*